Metformin attenuates the progression of esophageal squamous cell carcinoma by downregulating miR-141-3p to enhance SCEL

Abstract

Introduction

Metformin (Met), a first-line oral anti-type 2 diabetes medication used globally, has been shown to hinder cancer progression via regulation of microRNAs (miRNAs). The previous reports on the relationship between Met use and the risk of esophageal squamous cell carcinoma (ESCC) have been controversial. Hence, this study aimed to explore how Met affected ESCC progression and the underlying molecular mechanism.

Material and methods

Cell migration, viability and invasiveness were respectively investigated using wound healing, CCK-8 and transwell assay. The expressions of miR-141-3p and Sciellin (SCEL) mRNA were examined by mean of quantitative real-time PCR (qRT-PCR) assay, and SCEL protein level was quantified by western blotting. In vivo tests of Met were performed on animals. The predicted binding of miR-141-3p to SCEL was more evidenced by dual-luciferase assay.

Results

Met treatment in ESCC cell largely impaired cell viability, migration and invasiveness. MiR-141-3p showed high expression in ESCC and was downregulated in ESCC cells after Met treatment. MiR-141-3p upregulation in Met-administered ESCC cells largely restored cell proliferative ability, migration and invasiveness. MiR-141-3p also attenuated the anti-tumor effect of Met in vivo. MiR-141-3p targeted SCEL whose expression was declined in ESCC, and SCEL expression was reinforced in ESCC cells after Met treatment. MiR-141-3p upregulation depleted SCEL expression and thus partially abolished the anti-cancer impacts of SCEL in Met-treated ESCC cells.

Conclusions

Met restrains the progression of ESCC by regulating the miR-141-3p/SCEL axis. Our findings clearly show that Met is associated with a lower risk of ESCC, and its anticancer effect could potentially be used to treat ESCC.

Metformin attenuates the progression of esophageal squamous cell carcinoma by downregulating miR-141-3p to enhance SCEL

Running title: *Metformin blocks ESCC progression via miR-141-3p/SCEL axis*

Abstract

Background: Metformin (Met), a first-line oral anti-type 2 diabetes medication used globally, has been shown to hinder cancer progression via regulation of microRNAs (miRNAs). The previous reports on the relationship between Met use and the risk of esophageal squamous cell carcinoma (ESCC) have been controversial. Hence, this study aimed to explore how Met affected ESCC progression and the underlying molecular mechanism.

Material and methods: Cell migration, viability and invasiveness were respectively investigated using wound healing, CCK-8 and transwell assay. The expressions of miR-141-3p and Sciellin (SCEL) mRNA were examined by mean of quantitative real-time PCR (qRT-PCR) assay, and SCEL protein level was quantified by western blotting. *In vivo* tests of Met were performed on animals. The predicted binding of miR-141-3p to SCEL was more evidenced by dual-luciferase assay.

Results: Met treatment in ESCC cell largely impaired cell viability, migration and invasiveness. MiR-141-3p showed high expression in ESCC and was downregulated in ESCC cells after Met treatment. MiR-141-3p upregulation in Met-administered ESCC cells largely restored cell proliferative ability, migration and invasiveness. MiR-141-3p

also attenuated the anti-tumor effect of Met *in vivo*. MiR-141-3p targeted SCEL whose expression was declined in ESCC, and SCEL expression was reinforced in ESCC cells after Met treatment. MiR-141-3p upregulation depleted SCEL expression and thus partially abolished the anti-cancer impacts of SCEL in Met-treated ESCC cells.

Conclusion: Met restrains the progression of ESCC by regulating the miR-141-3p/SCEL axis. Our findings clearly show that Met is associated with a lower risk of ESCC, and its anticancer effect could potentially be used to treat ESCC.

Key words: Metformin, miR-141-3p, SCEL, ESCC

Introduction

The sixth most frequent type of cancer mortality globally is esophageal cancer [1]. In the last decade, we have witnessed that the treatment strategy for esophageal cancer has changed and new treatment modalities are replacing the traditional treatment of all stages of cancer, such as targeted therapies [2, 3]. Esophageal squamous cell carcinoma (ESCC) is the predominant histological type of esophageal cancer and is one of the most aggressive cancers of the gastrointestinal tract [1]. With a fewer than 20% patient 5-year survival rate, the prognosis for ESCC is quite bad [2]. Therefore, more new therapeutic strategies and agents are required to improve patients' outcomes.

Metformin (Met) is one of the drugs used for type 2 diabetes patients [4]. A series of epidemiological studies have shown a positive correlation between its use and lower cancer incidence and mortality rates [5]. The potential use of Met as an anticancer drug has been investigated in several research and clinical trials [6]. Patients using metformin had an overall reduced risk of ESCC compared to those not using metformin [7]. Although its potential use in cancer treatment has been investigated, however, there is still a great deal of uncertainty regarding the molecular mechanisms by which Met exerts its anticancer effects in ESCC.

Small non-coding RNAs called microRNAs (miRNAs) have short nucleotide lengths, and dysregulation of these RNAs participates in the onset and development of many diseases, especially cancer [8]. The considerable alterations of miRNA have been observed in numerous diseases after Met therapy [9, 10], implying that certain miRNAs may

participate in the regulation of Met in these diseases. For example, Met triggered ferroptosis to inhibit breast cancer progression by enriching miR-324-3p expression [11]. Met treatment increased miR-381 expression in lung cancer and then repressed cancer cell growth, migration and epithelial-mesenchymal transition (EMT) [12]. Interestingly, miR-141-3p was found to be downregulated in ESCC tissues and cells, and miR-141-3p knockdown in ESCC cells increased cell invasion, proliferation, and migration by activating the JAK2/STAT3 pathway [13]. Previous research has also demonstrated that miR-141-3p plays a role in Met-mediated inflammation and cancer progression [14, 15]. However, there is no evidence for the regulation of Met on miR-141-3p in ESCC progression.

MiRNAs are vital for the posttranscriptional regulation of gene expression [16]. Bioinformatics tool, such as TargetScan [17], predicts the binding sites between miRNA and mRNAs and thus provides potential target genes of indicated miRNA. Sciellin (SCEL), a precursor protein of cornified envelope, was demonstrated to block colorectal cancer cell migration and invasion [18]. It is predicted as a target downstream of miR-141-3p by TargetScan. Whereas, the interactions between miR-141-3p and SCEL in ESCC have not been unveiled.

In these contexts, we proposed the hypothesis that Met restrained the progression of ESCC via mediating miR-141-3p. We investigated miR-141-3p expression affected by Met in ESCC cells and its functions in Met-administered ESCC cells and animal models. We further testified the targets of miR-141-3p to further understand the molecular

mechanisms of Met in ESCC, so as to provide more strategies for ESCC therapy.

Materials and methods

Cell treatment

KYSE510 and KYSE140 purchased from BeNa Biotech (Beijing, China) were cultured in 90% RPMI1640 medium containing 10% FBS. Met purchased from Sigma-Aldrich (USA) was dissolved in PBS for further use. Met in PBS was added to culture KYSE510 and KYSE140 cells at the doses of 0 (blank PBS; control, CON), 5, 10, 20, 40, 80 and 160 mM.

CCK-8 assay

In 96-well plates, 3×10^3 cells/well treated cells were plated and cultivated for the required amount of time, such as 0, 24, 48, or 72 hours. After that, cells were dealt with CCK-8 reagent (10 μL/well) for additional 2 hours. The 450-nm absorbance of cells in each well was checked by a microplate reader (Molecular Device, Shanghai, China).

Wound healing assay

In 24-well plates, the treated cells were plated at a density of 5×10^4 cells per well, and they were subsequently grown until 90 percent of the cells had converged.Cell surface was created with an artificial wound using a sterile pipette tip. A microscope was used to swiftly record the wound's length (Nikon, Japan). The distance of wound healing was subsequently measured to assess cell migration after 24 hours of cell culture.

Transwell assay

Matrigel (BD Biosciences, USA)-coated transwell chambers were used here. The treated

cells were, in essence, collected, suspended in serum-free RPMI 1640 media, and then

moved to the upper filter of chambers. To encourage cell invasion, fresh RPMI1640

containing 20% FBS was introduced to the chamber bottoms. Cells that settled at the

bottom of the filter were preserved with methanol and colored with 0.1 percent crystal

violet 24 hours later. Under light microscopy, five randomly chosen fields were chosen to

count the number of invasive cells (Nikon).

Tissue sample collection

38 pairs of ESCC tumor samples and matched normal samples were acquired from our

hospital. Patients who had received pathological examination confirmation of primary

ESCC and had never been treated with any anti-cancer treatments prior to surgery were

included in this study. These patients provided written informed consent for sample

collection, and samples were all preserved at -80℃ conditions for different analyses.

These procedures were approved by the Ethics Committee of our hospital.

Quantitative real-time PCR (qRT-PCR)

Total RNA was isolated from the experimental samples using Trizol reagent (Invitrogen,

USA). Then, 1 μg of total RNA was reverse-transcribed into cDNA using PrimeScript RT

Reagent Kit (Takara, Dalian, China) or using miRNA miScript Reverse Transcription Kit

(Qiagen, Duesseldorf, Germany). Next, a SYBR Green Mix (Takara) was utilized to

quantify cDNA for qRT-PCR. All steps followed the guidelines of protocol. We adopted

GAPDH or U6 as the internal control and utilized the $2^{-\Delta\Delta CT}$ method to process results.

Primers sequences were exhibited in Table 1.

Cell transfections

MiR-141-3p mimic (mimic) and mimic negative control (mimic-NC) were obtained from RiboBio (Guangzhou, China). SCEL was overexpressed by using pcDNA3.1 vector, and SCEL overexpression vector (OE-SCEL) was constructed by Tsingke (Beijing, China), using empty vector as the control (OE-NC). The mimics or vectors were introduced into ESCC cells using a Lipofectamine 3000 reagent (Invitrogen) as protocol suggested. The transfection efficiency was checked at 24 h post-transfection using qRT-PCR.

Animal model construction

To induce tumorigenesis *in vivo*, KYSE140 cells were hypodermically inoculated into nude mice (2×10^6 cells per mouse; female) that were purchased from Vital River (Beijing, China). A total of 4 groups of experimental mice (n=5 per group) were included in this study, including CON group, Met group, Met+agomiR group and Met+agomiR-NC group. One week later, all tumor nodes were regularly developed. MiR-141-3p agomiR (5 nmol at a time) or agomiR-NC was intratumorally injected into tumors, and Met (250 mg/kg) or equal vehicle (PBS) was intraperitoneally injected into mice every three days. During this period, tumor volume (length×width^2×0.5) was weekly recorded. After 5 weeks, all tumor nodes were excised from nude mice when euthanized. Our hospital's Ethics Committee gave its approval for the usage of animals.

Dual-luciferase reporter assay

The predicted binding site of miR-141-3p to SCEL 3'UTR was obtained from TargetScan.

Then, the wild-type (WT) and mutant-type (MUT) sequences of SCEL were designed and synthesized by Tsingke, and the WT or MUT sequence of SCEL was inserted into pmirGLO vector to construct reporter vectors by Tsingke. The WT or MUT reporter vector of SCEL and miR-141-3p mimic (using mimic-NC as the control) were commonly introduced into ESCC cells. Using the Luciferase Reporter Assay System, luciferase activity were examined after sustaining cells for 48 hours (Promega, USA).

Western blotting

RIPA reagent (Solarbio, Beijing, China) was used to extract proteins from test samples and then used for quantification analysis using BCA kit (Solarbio). Protein samples (20 μg per lane) were loaded to 10% SDS-PAGE. After being separated, the proteins were put on PVDF membranes. The membranes were detected with the primary antibodies (anti-SCEL, ab197087, 1:500; Abcam, USA) at 4℃ overnight after blocking with 5% skim-milk at room temperature for 1 hour. Antibody of GAPDH (ab9485, 1:2500; Abcam) was applied as internal reference. Subsequently, the membranes were probed with matched HRP-labeled secondary antibody (ab205718, 1:20000; Abcam) for 2 hours. The enhanced chemiluminescence substrate from Solarbio was used to appear protein bands.

Statistical analysis

Data processing and data normality were analyzed using GraphPad Prism 7.0 (GraphPad, USA). Data from 3 independent experiments were exhibited as means ± standard deviation. The Student's t-test was used to compare two groups' differences, and analysis

of variance was used to compare more than two groups. *P* values of less than 0.05 were considered statistically significant.

Results

Met repressed ESCC cell viability, migration and invasion

Initially, we validated the effects of Met in ESCC cells. The chemical structural formula of Met was exhibited in Figure 1A. KYSE510 and KYSE140 cells were administered with different doses of Met, and their viability was markedly declined in a dose-dependent manner. We obtained that the IC50 of cells to Met was around 10 mM concentration of Met (Figure 1B) so that 10 mM concentration of Met was used for the following experiments. In addition, we monitored from wound healing assay that the wound healing distance of Met-treated cells was notably shorter than that of control-treated cells (Figure 1C). The data from transwell assay displayed that Met treatment strikingly weakened the number of invaded cells of KYSE510 and KYSE140 (Figure 1D). These phenotypes partly illustrated the anti-cancer effects of Met.

MiR-141-3p upregulation attenuated the anti-cancer effects of Met *in vitro*

Higher expression of miR-141-3p was observed in tumor tissues of ESCC in comparison to normal tissues (Figure 2A). Interestingly, miR-141-3p level was monitored to be weakened in Met-treated KYSE510 and KYSE140 cells relative to control cells (Figure 2B). These two cell lines were able to overexpress miR-141-3p when transfected with miR-141-3p mimic (Figure 2C). Next, KYSE510 and KYSE140 cells transfected with

miR-141-3p mimic or mimic-NC were administered with 10 mM Met. We observed that cancer cells overexpressing miR-141-3p had aggravated proliferative capacity (Figure 2D). Besides, relative to mimic-NC, miR-141-3p transfection strengthened KYSE510 and KYSE140 cell migratory and invasive phenotypes (Figure 2E and 2F). The outcomes manifested that miR-141-3p weakened the anti-cancer effect of Met and thus restored ESCC cell malignant phenotypes.

MiR-141-3p upregulation impaired the anti-tumor effect of Met *in vivo*

KYSE140 cells were hypodermically infused into nude mice to induce tumor formation in animal models. Then, miR-141-3p agomir or agomir-NC was intratumorally injected into tumors, and Met or vehicle (PBS) was intraperitoneally injected into mice every three days. As a result, we discovered that Met administration in mice resulted in smaller tumor size, volume and weight relative to control, while synchronous treatment of miR-141-3p agomir rather than agomir-NC substantially recovered tumor size, volume and weight (Figure 3A-3C), suggesting that miR-141-3p enrichment weakened the anti-tumor activity of Met *in vivo*.

MiR-141-3p bound to SCEL 3'UTR to sequester SCEL expression

The potential mRNAs targeted by miR-141-3p were predicted using TargetScan, and miR-141-3p was shown to possess a binding site on SCEL 3'UTR (Figure 4A). Then, miR-141-3p enrichment in KYSE510 and KYSE140 cells noticeably reduced luciferase activities of SCEL WT constructs, while miR-141-3p enrichment in cells could not reduce luciferase activities of SCEL MUT constructs (Figure 4B). SCEL expression was

strikingly poorer in ESCC tumor samples in contrast to normal samples (Figure 4C), which showed inverse correlation with miR-141-3p expression in ESCC samples (Figure 4D). Interestingly, SCEL expression was markedly elevated in Met-administered KYSE510 and KYSE140 cells (Figure 4E). We further determined that SCEL mRNA and protein were notably reinforced in KYSE510 and KYSE140 cells with infection of OE-SCEL but largely decreased in cells with transfection of mimic, and its expressions were substantially repressed by OE-SCEL+mimic relative to OE-SCEL in cells (Figure 4F and 4G), revealing that miR-141-3p targeted SCEL to deplete SCEL expression.

MiR-141-3p enrichment attenuated the anti-cancer effects of Met *in vitro* by downregulating SCEL

KYSE510 and SYSE140 cells after introduction of OE-SCEL, miR-141-3p mimic, or OE-SCEL+mimic were administered with Met to observe the function of SCEL and the interactions of miR-141-3p and SCEL. In function, SCEL upregulation showed the opposite effects with miR-141-3p, showing that SCEL overexpression in KYSE510 and KYSE140 cells strengthened Met effects and further impaired cell proliferation, migratory and invasive abilities (Figure 5A-5C). However, these suppressive cell phenotypes were largely reverted in SCEL-overexpressed cells with co-transfected with miR-141-3p mimic (Figure 5A-5C). We concluded that miR-141-3p reintroduction decreased SCEL expression and thus attenuated the anti-cancer effects of Met.

Discussion

Our work unveiled the mechanism of anti-diabetes drug, Met, in ESCC through the perspective of miRNA regulation. MiR-141-3p was overly expressed in ESCC, while it was downregulated in ESCC after Met treatment. The anti-cancer potency of Met was attenuated by miR-141-3p upregulation. MiR-141-3p targeted SCEL that was poorly expressed in ESCC. Met strengthened the expression of SCEL in ESCC, and SCEL overexpression enhanced the anti-cancer potency of Met. Our results indicated that Met repressed ESCC progression via modulating miR-141-3p/SCEL pathway.

Met administration suppressed breast cancer cell invasion, migration and adhesion via downregulating VEGF and MMP9, however the authors did not elaborate on the precise molecular mechanism [19]. Met was demonstrated to enhance apoptosis and impede growth, invasion and EMT in ESCC cells, and it also strengthened the chemosensitivity of cisplatin in ESCC [20-22], verifying the regulatory functions of Met on ESCC development. Consistent with these outcomes, we testified that the viability, migratory and invasive abilities of ESCC cells were remarkably repressed after Met treatment. Given that Met was previously shown to trigger ESCC cell pyroptosis via modulating the miR-497/PELP1 axis [23], we insisted that Met might affect ESCC progression via other miRNA/mRNA pathways.

MiR-141-3p was reported to be overly expressed in ESCC [13, 24]. Inhibition of miR-141-3p in ESCC cells reinforced autophagy and impaired proliferative, migratory and invasive activities [24]. MiR-141-3p was also highly regulated in cisplatin-resistant ESCC cells relative to cisplatin-sensitive ESCC cells, and miR-141-3p overexpression

prevented cisplatin-induced cell apoptosis and thus conferred ESCC chemoresistance [25]. The data highlighted the oncogenic role of miR-141-3p in ESCC. Interestingly, Docrat et al. published that Met usage alleviated neuroinflammation via decreasing miR-141-3p expression in diabetic mice [14], which illustrated the implication of miR-141-3p in Met-mediated biological processes. Consistent with the previous findings, we observed that miR-141-3p level of expression was greatly diminished by Met treatment in ESCC cells. MiR-141-3p enrichment hindered the anti-cancer effects of Met, thereby recovering ESCC cell proliferative, migratory and invasive abilities, as well as tumor development *in vivo*. Our perspective emphasized the usefulness of miR-141-3p-targeted inhibition for enhancing the anti-cancer effects of Met.

In our findings, the miR-141-association 3p's with SCEL was confirmed. In view of the deficiency of SCEL functions in ESCC, we selected SCEL as a study object. We testified the decreased expression of SCEL in ESCC. Similarly, SCEL expression was also downregulated in colorectal cancer and showed the repressive effects on colorectal cancer cell migration and invasion [18]. We characterized that SCEL expression was remarkably enhanced in ESCC cells after Met treatment. SCEL overexpression strengthened the anti-cancer impacts of Met, leading to further inhibition of cell proliferation, migration and invasion. But miR-141-3p coupled to SCEL and inhibited SCEL expression, partially removing SCEL's functional functions. The data revealed that miR-141-3p/SCEL axis was governed by Met in ESCC.

Interestingly, it has been noted by several groups that Met can alter the epigenetic

landscape of cells and influence the expression of multiple genes across the genomes[26, 27]. It is therefore possible that the regulation of miR-141-3p by Met could have an epigenetic mechanism. However, given that any potential effect of Met on cellular epigenetics will be genome wide, it was not explored in the present study which is quite specific to miR-141-3p and its effect on SCEL. This, however, could be a very interesting avenue of investigation for future work. Apart from this, there are some other limitations to our study. For example, numerous miRNAs might be influenced by Met, and we only focused on miR-141-3p. More miRNAs regulated by Met should be further identified. In addition, miR-141-3p had numerous target genes, and several of them might be involved in Met-mediated miR-141-3p networks. Other targets should be explored in future work.

Conclusion

Here, we testified that Met played anti-cancer effects in ESCC. Met decreased the expression of miR-141-3p in ESCC, and miR-141-3p upregulation attenuated the efficiency of Met. Moreover, miR-141-3p directly targeted SCEL whose expression was elevated by Met. Thus, we concluded that Met restrained ESCC development via mediating the miR-141-3p/SCEL axis, which extended the understanding of molecular mechanisms by which Met exerts its anticancer impact in ESCC.

Declarations

Funding

No funding was received.

Conflicts of interest

The authors affirm that they do not have any competing interests.

Ethics approval

Our hospital's Ethics Committee gave its approval to the current study (Wuhan, China).

The Declaration of Helsinki's ethical guidelines are strictly followed when processing

clinical tissue samples. Each patient completed an informed consent form in writing.

Our hospital's Ethics Committee gave its approval for this animal experiment, which was

carried out in compliance with the ARRIVE criteria.

Consent to participate

All patients signed written informed consent.

Consent for publication

Participants gave their permission for their names to be published.

Availability of data and material

This article contains all of the data that were created or examined during this investigation.

Authors' contributions

The experiments were run and the data was analyzed by SL and TYC. The study was created and planned by SL. The data were acquired by SL and FYJ. The data were analyzed and interpreted by TYC and FYJ. The article was reviewed and approved by all authors.

Acknowledgements

None.

References

[1]   Sung H, Ferlay J, Siegel RL, et al. Global Cancer Statistics 2020: GLOBOCAN Estimates of Incidence and Mortality Worldwide for 36 Cancers in 185 Countries. CA: a cancer journal for clinicians. 2021;71(3):209-49.

[2]   Kadian LK, Arora M, Prasad CP, Pramanik R, Chauhan SS. Signaling pathways and their potential therapeutic utility in esophageal squamous cell carcinoma. Clinical & translational oncology : official publication of the Federation of Spanish Oncology Societies and of the National Cancer Institute of Mexico. 2022;24(6):1014-32.

[3]   Gullotta F. [Neuropathological findings in aminoaciduria (maple syrup disease; tyrosinosis)]. Pathologica. 1971;63(915):9-15.

[4]   Sanchez-Rangel E, Inzucchi SE. Metformin: clinical use in type 2 diabetes. Diabetologia. 2017;60(9):1586-93.

[5]   Ahmed ZSO, Golovoy M, Abdullah Y, Ahmed RSI, Dou QP. Repurposing of Metformin for Cancer Therapy: Updated Patent and Literature Review. Recent patents on anti-cancer drug discovery. 2021;16(2):161-86.

[6]   Vancura A, Bu P, Bhagwat M, Zeng J, Vancurova I. Metformin as an Anticancer Agent. Trends in pharmacological sciences. 2018;39(10):867-78.

[7]   Wang QL, Santoni G, Ness-Jensen E, Lagergren J, Xie SH. Association Between Metformin Use and Risk of Esophageal Squamous Cell Carcinoma in a Population-Based Cohort Study. The American journal of gastroenterology. 2020;115(1):73-8.

[8]   He B, Zhao Z, Cai Q, et al. miRNA-based biomarkers, therapies, and resistance in Cancer. International journal of biological sciences. 2020;16(14):2628-47.

[9]   Alimoradi N, Firouzabadi N, Fatehi R. Metformin and insulin-resistant related diseases: Emphasis on the role of microRNAs. Biomedicine & pharmacotherapy = Biomedecine & pharmacotherapie. 2021;139:111662.

[10] Alimoradi N, Firouzabadi N, Fatehi R. How metformin affects various malignancies by means of microRNAs: a brief review. Cancer cell international. 2021;21(1):207.

[11] Hou Y, Cai S, Yu S, Lin H. Metformin induces ferroptosis by targeting miR-324-3p/GPX4 axis in breast cancer. Acta biochimica et biophysica Sinica. 2021;53(3):333-41.

[12] Jin D, Guo J, Wu Y, et al. Metformin-repressed miR-381-YAP-snail axis activity disrupts NSCLC growth and metastasis. Journal of experimental & clinical cancer research : CR. 2020;39(1):6.

[13] Ishibashi O, Akagi I, Ogawa Y, Inui T. MiR-141-3p is upregulated in esophageal squamous cell carcinoma and targets pleckstrin homology domain leucine-rich repeat protein phosphatase-2, a negative regulator of the PI3K/AKT pathway. Biochemical and biophysical research communications. 2018;501(2):507-13.

[14] Docrat TF, Nagiah S, Chuturgoon AA. Metformin protects against neuroinflammation through integrated mechanisms of miR-141 and the NF-κB-mediated inflammasome pathway in a diabetic mouse model. European journal of pharmacology. 2021;903:174146.

[15] Chen D, Chou FJ, Chen Y, et al. Targeting the radiation-induced TR4 nuclear receptor-mediated QKI/circZEB1/miR-141-3p/ZEB1 signaling increases prostate cancer radiosensitivity. Cancer letters. 2020;495:100-11.

[16] Rani V, Sengar RS. Biogenesis and mechanisms of microRNA-mediated gene regulation.

Biotechnology and bioengineering. 2022;119(3):685-92.

[17] Agarwal V, Bell GW, Nam JW, Bartel DP. Predicting effective microRNA target sites in mammalian mRNAs. eLife. 2015;4.

[18] Chou CK, Fan CC, Lin PS, et al. Sciellin mediates mesenchymal-to-epithelial transition in colorectal cancer hepatic metastasis. Oncotarget. 2016;7(18):25742-54.

[19] Farahi A, Abedini MR, Javdani H, et al. Crocin and Metformin suppress metastatic breast cancer progression via VEGF and MMP9 downregulations: in vitro and in vivo studies. Molecular and cellular biochemistry. 2021;476(9):3341-51.

[20] Sekino N, Kano M, Matsumoto Y, et al. Antitumor effects of metformin are a result of inhibiting nuclear factor kappa B nuclear translocation in esophageal squamous cell carcinoma. Cancer science. 2018;109(4):1066-74.

[21] Liang F, Wang YG, Wang C. Metformin Inhibited Growth, Invasion and Metastasis of Esophageal Squamous Cell Carcinoma in Vitro and in Vivo. Cellular physiology and biochemistry : international journal of experimental cellular physiology, biochemistry, and pharmacology. 2018;51(3):1276-86.

[22] Wang F, Ding X, Wang T, et al. Metformin inhibited esophageal squamous cell carcinoma proliferation in vitro and in vivo and enhanced the anti-cancer effect of cisplatin. PloS one. 2017;12(4):e0174276.

[23] Wang L, Li K, Lin X, et al. Metformin induces human esophageal carcinoma cell pyroptosis by targeting the miR-497/PELP1 axis. Cancer letters. 2019;450:22-31.

[24] Phatak P, Noe M, Asrani K, Chesnick IE, Greenwald BD, Donahue JM. MicroRNA-141-3p regulates cellular proliferation, migration, and invasion in esophageal cancer by targeting tuberous sclerosis complex 1. Molecular carcinogenesis. 2021;60(2):125-37.

[25] Imanaka Y, Tsuchiya S, Sato F, Shimada Y, Shimizu K, Tsujimoto G. MicroRNA-141 confers resistance to cisplatin-induced apoptosis by targeting YAP1 in human esophageal squamous cell carcinoma. Journal of human genetics. 2011;56(4):270-6.

[26] Bridgeman SC, Ellison GC, Melton PE, Newsholme P, Mamotte CDS. Epigenetic effects of metformin: From molecular mechanisms to clinical implications. Diabetes Obes Metab. 2018;20(7):1553-62.

[27] Menendez JA. Metformin: Sentinel of the Epigenetic Landscapes That Underlie Cell Fate and Identity. Biomolecules. 2020;10(5).

Figure legends

Figure 1 Met restrained ESCC cell viability, migration and invasion. (A) The chemical structural formula of Met. (B) Cell viability of KYSE510 and KYSE140 cells with the treatment of different doses of Met was checked by CCK-8 assay. (C) Cell migration of cells treated with Met or control was evaluated by wound healing assay. (D) Cell invasion of cells treated with Met or control was evaluated by transwell assay. $*P<0.05$ and $**P<0.01$ vs CON.
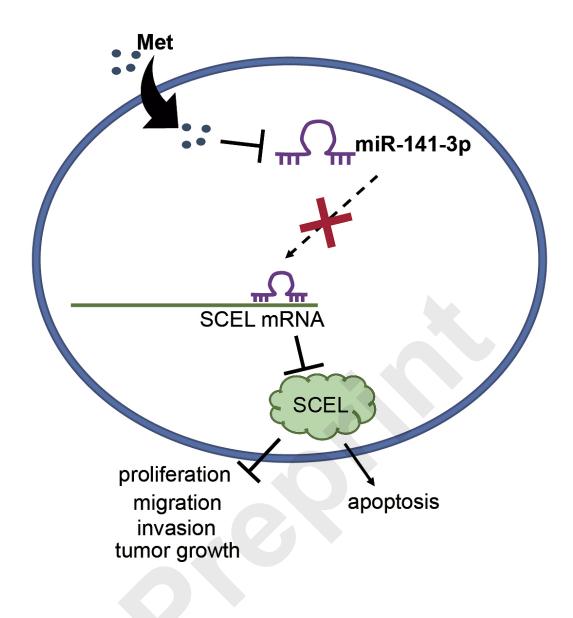
Figure 2 Met depleted miR-141-3p expression to restrain ESCC cell malignant phenotypes. (A) MiR-141-3p expression in tumor and normal samples was determined by qRT-PCR. (B) MiR-141-3p expression in KYSE510 and KYSE140 cells treated with Met or CON was examined by qRT-PCR, $**P<0.01$ vs CON. (C) The efficiency of miR-141-3p mimic was checked by qRT-PCR. (D-F) KYSE510 and KYSE140 cells transfected with miR-141-3p mimic or mimic-NC were treated with Met or CON. (D) Cell proliferative capacity was assessed by CCK-8 assay. (E) Cell migratory capacity was assessed by wound healing assay. (F) Cell invasive capacity was assessed by transwell assay. $**P<0.01$ vs mimic-NC.

Figure 3 Met depleted miR-141-3p expression to restrain tumor development *in vivo*. (A-C) Animal models included 4 groups, CON-administered group, Met-administered group, Met+miR-141-3p agomiR-administered group, and Met+agomiR-NC-

administered group. (A) Representative tumor tissues isolated from animal models. (B) Tumor volume was weekly recorded during tumor growth. (C) Tumor weight was measured after excising from animal models after 5 weeks. **$P<0.01$.

Figure 4 MiR-141-3p bound to SCEL 3'UTR to sequester SCEL expression. (A) The predicted binding site between miR-141-3p and SCEL 3'UTR was obtained from TargetScan. (B) The putative binding site was verified by dual-luciferase reporter assays, **$P<0.01$ vs miR-NC. (C) SCEL expression in tumor and normal samples was checked by qRT-PCR. (D) The correlation between SCEL expression and miR-141-3p expression in tumor samples was analyzed by Spearman's analysis. (E) SCEL mRNA expression in KYSE510 and KYSE140 cells treated with Met or CON was examined by qRT-PCR, **$P<0.01$ vs CON. (F and G) KYSE mRNA expression (F) and protein expression (G) in KYSE510 and KYSE140 cells transfected with OE-SCEL, miR-141-3p mimic, or OE-SCEL+mimic were checked by qRT-PCR and western blotting, **$P<0.01$ vs OE-NC; ##$P<0.01$ vs mimic-NC; &&$P<0.01$ vs OE-SCEL+mimic.

Figure 5 MiR-141-3p suppressed SCEL expression to recover KYSE510 and KYSE140 cell malignant phenotypes in Met-treated cells. (A-C) KYSE510 and KYSE140 cells transfected with OE-SCEL, OE-NC, miR-141-3p mimic, mimic-NC, or OE-SCEL+mimic were administered with 10 nM Met. (A) Cell proliferation was evaluated by CCK-8 assay. (B) Cell migration was evaluated by wound healing assay. (C)

Cell invasion was evaluated by transwell assay. $*P<0.05$ and $**P<0.01$ vs OE-NC; $^{#}P<0.05$ and $^{##}P<0.01$ vs mimic-NC; $^{&}P<0.05$ and $^{&&}P<0.01$ vs OE-SCEL+mimic.

Table 1 qRT-PCR Primer sequences

Gene		Sequences
miR-141-3p	Forward	5′-GCGCGTAACACTGTCTGGTAA-3′
	Reverse	5′-AGTGCAGGGTCCGAGGTATT-3′
SCEL	Forward	5′-GGTGGTGCTCAACCGACATA-3′
	Reverse	5′-GGAAACCAGGACTGCCTCTT-3′
U6	Forward	5′ -CTCGCTTCGGCAGCACA-3′
	Reverse	5′ -AACGCTTCACGAATTTGCGT-3′
GAPDH	Forward	5′ -AGAAAAACCTGCCAAATATGATGAC-3′
	Reverse	5′ -TGGGTGTCGCTGTTGAAGTC-3′

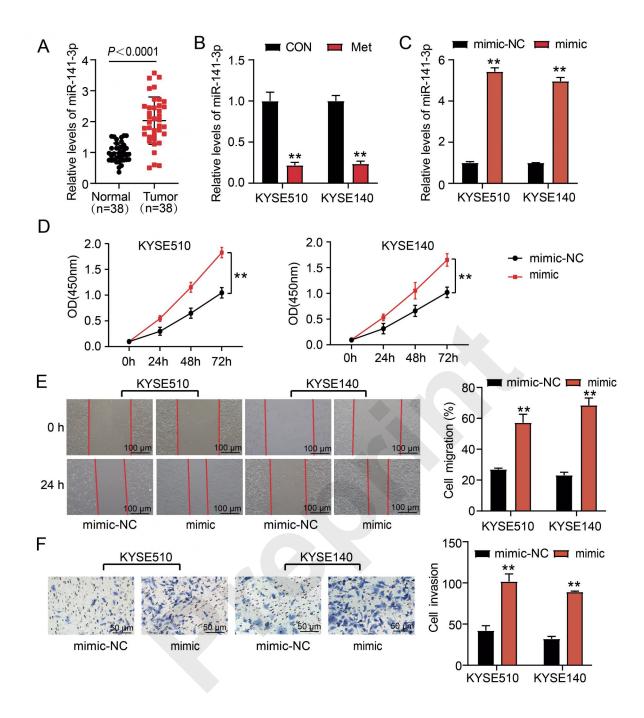Figure 1 Met restrained ESCC cell viability, migration and invasion.

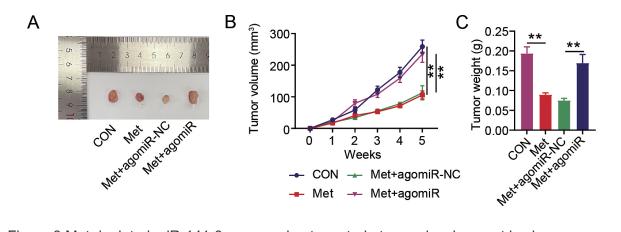Figure 2 Met depleted miR-141-3p expression to restrain ESCC cell malignant phenotypes.

Figure 3 Met depleted miR-141-3p expression to restrain tumor development in vivo.

A

Position 1421-1427 of SCEL 3'UTR   5'...AAGCCUGGUUCACAAAGUGUUAA...3'

⎸⎸⎸⎸⎸⎸⎸

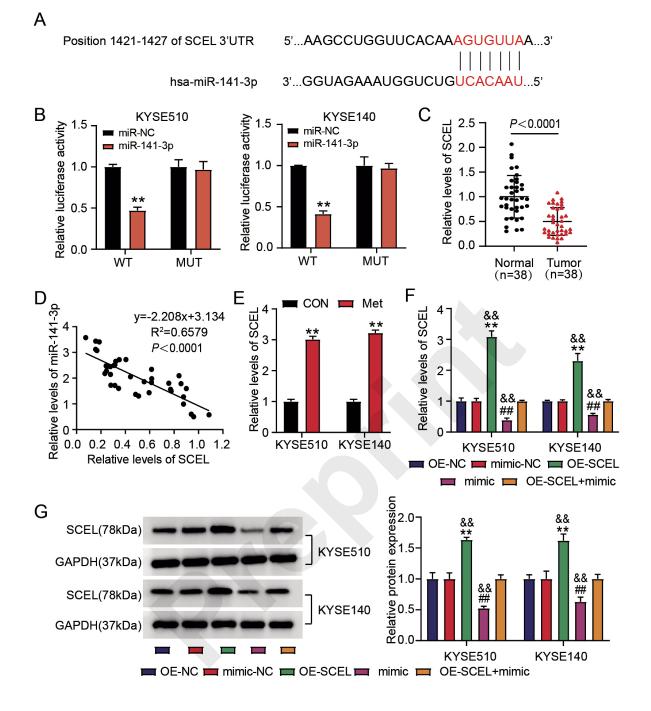hsa-miR-141-3p   3'...GGUAGAAAUGGUCUGUCACAAU...5'

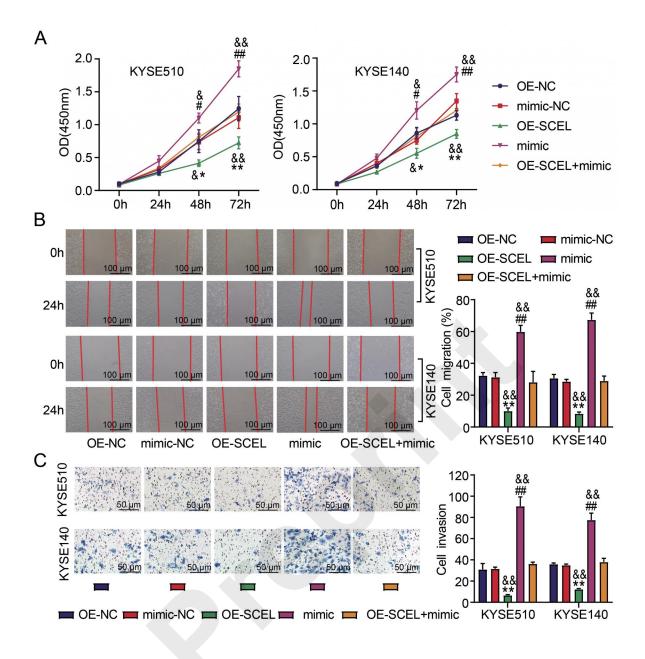Figure 4 MiR-141-3p bound to SCEL 3'UTR to sequester SCEL expression.

Figure 5 MiR-141-3p suppressed SCEL expression to recover KYSE510 and KYSE140 cell malignant phenotypes in Met-treated cells.